Electrochimica Acta 58 (2011) 179–183

Contents lists available at SciVerse ScienceDirect

Electrochimica Acta

journal homepage: www.elsevier.com/locate/electacta

Direct electrochemistry of glucose oxidase and biosensing for glucose based on helical carbon nanotubes modified magnetic electrodes

Rongjing Cui[a,c], Zhida Han[a], Jie Pan[a], E.S. Abdel-Halim[b], Jun-Jie Zhu[c,*]

[a] Jiangsu Laboratory of Advanced Functional Materials, Changshu Institute of Technology, Changshu 215500, China
[b] Petrochemical Research Chair, Chemistry Department, College of Science, King Saud University, P.O. Box 2455, Riyadh 11451, Saudi Arabia
[c] State Key Lab of Analytical Chemistry for Life Science, School of Chemistry, Chemical Engineering, Nanjing University, Nanjing 210093, China

ARTICLE INFO

Article history:
Received 24 June 2011
Received in revised form
11 September 2011
Accepted 13 September 2011
Available online 21 September 2011

Keywords:
Helical carbon nanotubes
Glucose oxidase
Biosensor
Magnetic electrode

ABSTRACT

Poly(diallyldimethylammonium chloride) functionalized helical carbon nanotubes (PDDA-HCNTs) were successfully synthesized. The resulting PDDA-HCNTs composite has good conductivity, solubility and ferromagnetic property. The fabricated HCNTs could be conveniently separated and magnetically attached to the magnetic electrode owing to their excellent magnetic properties. An amperometric biosensor was firstly developed based on glucose oxidase (GOD) functionalized PDDA-HCNTs loaded on magnetic glass carbon electrode. The constructed biosensor exhibited excellent electrocatalytic activity and stability for the detection of glucose with a linear range from 5 to 85 μM and a low detection limit of 0.72 μM at 3σ. The present work offers a new avenue to broaden the applications of HCNTs in electrochemical biosensors.

1. Introduction

Biosensors have attracted much attention in recent years due to their potential applications in clinical diagnostics, environmental monitoring, pharmaceuticals, food processing industries, and because of their fast response and ease of operation modes. The key step in the development of biosensors is the effective immobilization of enzyme on the electrode surface. Many kinds of nanoparticles such as Ag [1], Au [2,3], Pt [4], carbon nanotubes (CNTs) [5–7] and semiconductor (CdSe/ZnS) [8] have been reported for the immobilization of enzyme in the fabrication of biosensors. Despite many advances in these fields, it is still a challenge to find some new materials and methods to improve the simplicity, selectivity, and sensitivity [9].

Helical carbon nanotubes (HCNTs) were first predicted in 1993 by Itoh et al. [10] and were first observed in 1994 by Zhang et al. [11,12]. Because the HCNTs have a particular 3D-helical structure, they have unique characteristics, such as high superelastic property [13], high electromagnetic waves absorption [10], stereospecific nature of magnetoresistance [11], high hydrogen absorption [12], etc. Tang et al. reported the synthesis of HCNTs in the pyrolysis of acetylene at 450 °C over Fe nanoparticles generated by a combined sol–gel/reduction method [14,15]. Compared with straight CNTs, the as-prepared HCNTs have a specific helical structure, and more importantly, some ferromagnetic iron species can be found to be encapsulated in the HCNTs, which may favor electron transfer and facilitate catalytic activity. However, the reports on their electrocatalytic characteristic of HCNTs are rather rare perhaps due to their poor solubility in water.

In this work, PDDA was used to noncovalently functionalize HCNTs in order to increase the solubility to extend the application in biosensing. The fabricated PDDA-HCNTs could be conveniently separated and magnetically loaded on the working electrode owing to their excellent magnetic properties. In particular, PDDA-HCNTs provided a positively charged substrate for the immobilization of low isoelectric point (IEP) enzyme such as glucose oxidase (GOD) (IEP ≈ 4.2) at the physiological pH of 7.4. Herein, an amperometric biosensor was developed based on GOD functionalized PDDA-HCNTs loaded on magnetic glass carbon electrode (MGCE). The constructed biosensor displayed a fast electron transfer and a good electrochemistry activity for the detection of glucose with high stability and low detection limit. Therefore, the present work offers a new avenue to broaden the applications of HCNTs in electrochemical biosensors.

2. Experimental

2.1. Materials and apparatus

Glucose, glucose oxidase type VII (136,000 units/g, EC 1.1.3.4. from *Aspergillus niger*) and PDDA (MW = 200,000–350,000) were from Sigma. $FeCl_2 \cdot 4H_2O$, citric acid monohydrate and ethanol were

* Corresponding author. Fax: +86 25 83594976.
E-mail address: jjzhu@nju.edu.cn (J.-J. Zhu).

0013-4686/$ – see front matter © 2011 Elsevier Ltd. All rights reserved.
doi:10.1016/j.electacta.2011.09.030

from Nanjing Reagent Co. (Nanjing, China). The electrochemical impedance spectroscopy analyses were performed with an Autolab PGSTAT12 (Eco chemie, BV, The Netherlands) and controlled by GPES 4.9 and FRA 4.9 softwares. The electrochemical impedance spectra were recorded in the frequency range $0.1 \sim 1.0 \times 10^5$ Hz, at the formal potential of the $[Fe(CN)_6]^{3-/4-}$ redox couple and with a perturbation potential of 5 mV. Electrochemical measurements were performed on a CHI 660D workstation (Shanghai Chenhua, China) with a conventional three electrode system comprised of a platinum wire auxiliary, a saturated calomel reference and the modified magnetic glass carbon working electrode. Characteristics were performed via field-emission scanning electron microscopy (FESEM, HITACHI S4800), high resolution transmission electron microscopy (HRTEM, JEOL 2010), zeta potential (ξ) of HCNTs and PDDA-HCNTs were measured in pure water on a Malven Nano-Z instrument. Magnetic measurements were carried out using a Lakeshore 7300 vibrating sample magnetometer (VSM) under a magnetic field up to 10 kOe.

2.2. Typical synthesis of HCNTs

In a typical experiment [14], 0.01 mol $FeCl_2 \cdot 4H_2O$ and 0.015 mol citric acid monohydrate were dissolved in 100 mL of ethanol absolute and stirred at 60 °C for 6 h. After being dried at 80 °C, the xerogel was heated at 450 °C for 3 h in air and turned into ferric oxide. 163 mg of ferric oxide powder was spread on a ceramic plate, which was placed in a quartz reaction tube (5 cm inner diameter and 35 cm in length). This assembly was laid in a stainless steel reaction tube of 5.2 cm inner diameter and 80 cm in length (equipped with temperature and gas-flow controls). Therefore, the iron oxide was reduced in H_2 at 425 °C for 4 h, and the acetylene decomposition was conducted at 475 °C for 2 h at atmospheric pressure over the Fe catalyst. After the system was cooled to room temperature, the as-prepared sample was obtained.

2.3. Preparation of soluble HCNTs

The HCNTs were functionalized with PDDA according to the following procedures: 5 mg/mL HCNTs were dispersed into a 0.10% PDDA aqueous solution containing 0.5 M NaCl and the resulting dispersion was sonicated for 30 min to give a homogeneous black suspension. Residual PDDA polymer was removed by magnetic separation and the complex was rinsed with water for at least three times. The collected PDDA-HCNTs were redispersed in water with mild sonication to produce a stable solution, and then that solution was sonicated for 5 min immediately before preparing the films.

2.4. Fabrication of the GOD–PDDA-HCNTs/MGCE biosensor

The MGCE was first polished with 0.3 and 0.05 μm alumina slurry, and sonicated in ethanol and water successively. In succession, the 3 mg/mL of GOD stock solution (1) was mixed with the 4 mg/mL of PDDA-HCNTs solution (2) (V1:V2 = 2:1) to form a stabled solution. Finally, 15 μL of mixed solution was added

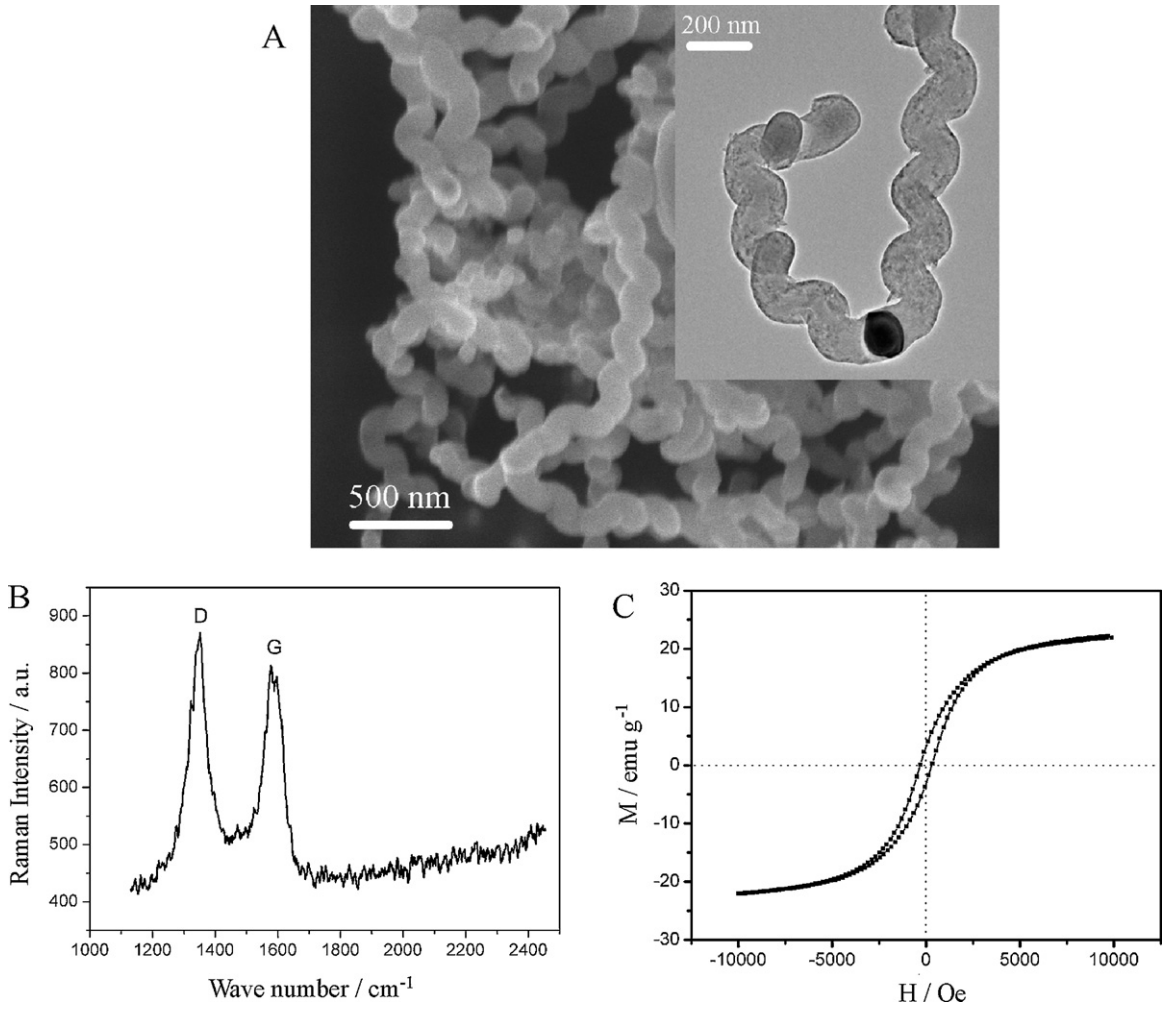

Fig. 1. (A) Typical FESEM image of the PDDA-HCNTs, (B) Raman spectra and (C) magnetization curve of the PDDA-HCNTs. Inset: TEM image of the PDDA-HCNTs.

dropwise onto MGCE dried at room temperature and stored at 4 °C before use. The magnetic electrode eliminates the possible fouling and prevents the leaching of the enzyme. When not in use, the GOD/PDDA-HCNTs/MGCE biosensor was stored in PBS at 4 °C. The electrochemical experiments were carried with a conventional three-electrode configuration.

3. Results and discussion

3.1. Characterization of PDDA-HCNTs

HCNTs were synthesized in the pyrolysis of acetylene at 475 °C over Fe nanoparticles generated by means of a combined sol–gel/reduction method. The cationic polyelectrolyte PDDA was used to noncovalently functionalize HCNTs in order to increase the solubility to extend the application in biosensing. Since the prepared HCNTs in aqueous solution (pH = 7.0) has a negative ξ-potential of −15.1 mV, the HCNTs are negatively charged and are electrostatically attracted to PDDA. The presence of a layer of adsorbed positively charged PDDA on the HCNTs caused a reversal in ξ-potential to positive value (+56.5 mV). The results demonstrated that PDDA provided a homogeneous distribution of positive charges on the surface of the HCNTs.

Fig. 1A shows FESEM images of the PDDA-HCNTs. The tubes range from 150 to 200 nm in diameter and most tubes are coiled in a regular and tight fashion with a very short coil pitch. The image in the inset of Fig. 1A displays typical TEM image of PDDA-HCNTs. Double-HCNT structures and the nozzles of the tubes are clearly visible. The TEM image shows the growth of two coiled nanotubes from a catalyst nanoparticle. The catalyst nanoparticle has a grain size of ca. 80 nm and is wrapped by several layers of carbon at the node. Double-HCNT structures and the nozzles of the tubes are clearly visible.

Fig. 1B shows the Raman spectrum of the as-prepared PDDA-HCNTs sample. Two peaks are observed at ca. 1349.3 and 1580.1 cm^{-1}; the former is stronger than the latter. It is well known that crystalline graphite (such as highly oriented pyrolitic graphite) has a characteristic Raman peak at 1580 cm^{-1} (called the G-band), whereas disorder in carbon materials gives rise to an intense "defect-induced" band at 1350 cm^{-1} (called the D-band) [16]. For the PDDA-HCNTs, the observation of the D-band as well as its broad profile (full width at half maximum is 61.0 cm^{-1}) provides evidence for the presence of disorder and/or distortions in the sample. Fig. 1C shows the magnetization curve ($M-H$) for the PDDA-HCNTs sample measured at 300 K. The saturation magnetization (M_S) and the coercivity (H_c) of the as-prepared sample are 22.0 emu g^{-1} and 308.1 Oe, respectively. The result suggested that the nanomaterials possess excellent magnetic property, which is an advantage to their bioassay applications.

3.2. Direct electrochemistry of GOD immobilized on the PDDA-HCNTs/MGCE

Fig. 2A exhibits the schematic of glucose detection by electrochemical method by using GOD–PDDA-HCNTs modified MGCE. Electrochemical impedance spectroscopy (EIS) was reported as an effective method to monitor the feature of surface allowing the understanding of chemical transformation and processes associated with the conductive electrode surface. Fig. 2B shows the Nyquist plots of EIS for the bare MGCE, PDDA-HCNTs/MGCE and GOD–PDDA-HCNTs/MGCE. At a bare MGCE, the redox process of the $[Fe(CN)_6]^{3-/4-}$ probe showed an electron transfer resistance of about 2700 Ω (curve a); The PDDA-HCNTs modified MGCE showed a much lower resistance for the redox probe (curve b), implying that PDDA-HCNTs were an excellent electric conducting material

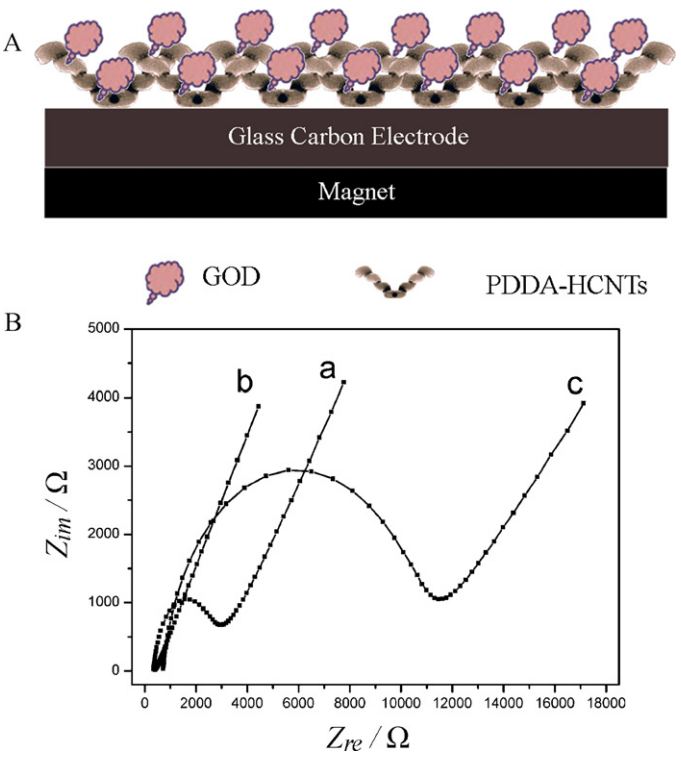

Fig. 2. (A) Schematic of glucose detection by electrochemical method using PDDA-HCNTs modified MGCE. (B) EIS of bare (a), PDDA-HCNTs (b), and GOD–PDDA-HCNTs (c) modified MGCE in 0.10 M KCl containing 5.0 mM $K_3[Fe(CN)_6]/K_4[Fe(CN)_6]$.

and accelerated the electron transfer. After GOD was coated on the PDDA-HCNTs/MGCE, the resistance increased dramatically to about 10^4 Ω (curve c), suggesting that the bulky GOD molecules blocked the electron exchange between the redox probe and electrode surface.

The direct electrochemistry of GOD immobilized on the PDDA-HCNTs/MGCE and MGCE were investigated. As shown in Fig. 3A, the cyclic voltammogram (CV) of the PDDA-HCNTs modified MGCE shows a weak reduction peak at −0.361 V in spite of the unobvious oxidation peak (curve a). The results can be attributed to ferromagnetic iron species encapsulated in the HCNTs. After combining with GOD, a pair of well-defined, quasireversible redox peaks can be observed at GOD–PDDA-HCNTs/MGCE at −0.491 V and −0.462 V (curve b), with a peak-to-peak separation of about 29 mV, revealing a fast electron transfer for the GOD Fe^{III}/Fe^{II} redox pair. In contrast, no obvious redox peaks were observed on the GOD/MGCE (curve c). These results demonstrated that the GOD–PDDA-HCNTs/MGCE retained high electrocatalytic activity, which attributed to the excellent conductivity and biocompatibility of PDDA-HCNTs.

The effect of scan rate was shown in Fig. 3B. With an increasing scan rate, the redox peak currents increased simultaneously, accompanied enlarged the peak separation. Moreover, both the cathodic and anodic peak currents increased linearly with the scan rate from 50 to 500 mV/s (inset of Fig. 3B), indicating a surface-controlled quasi-reversible process. According to Faraday's law, the surface concentration of electroactive GOD (Γ^*) at GOD–PDDA-HCNTs/MGCE was estimated to be 1.36×10^{-10} mol cm^{-2}, which was much larger than that (2.86×10^{-12} mol cm^{-2}) at the bare GCE [17]. This indicates that the PDDA-HCNTs modified electrode is much favorable for the immobilization of GOD because of its 3D-helical structure. PDDA-HCNTs provide a positively charged substrate for the immobilization of GOD (IEP ≈ 4.2) at the physiological pH of 7.4. Furthermore, GOD functionalized PDDA-HCNTs hybrids can be magnetically loaded on the magnetic working

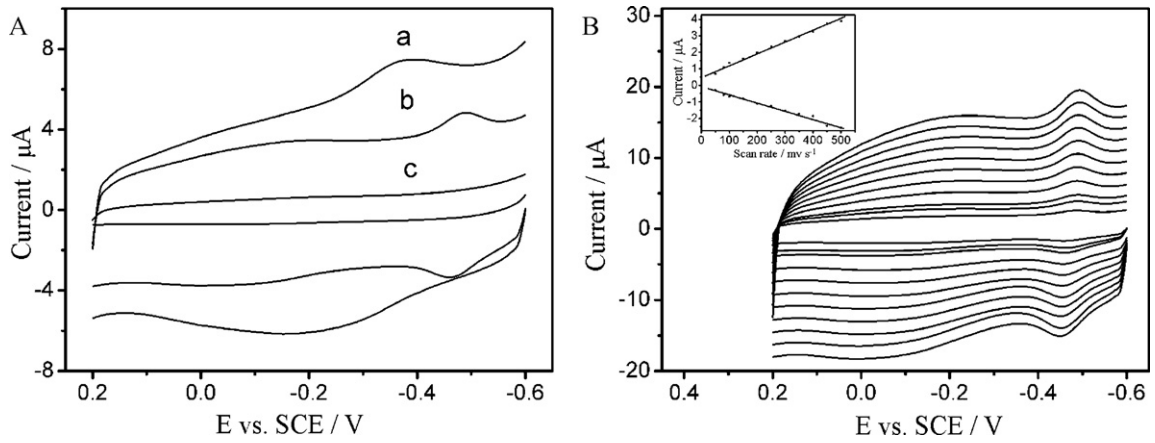

Fig. 3. (A) The CVs of different electrodes in nitrogen-saturated 0.1 M PBS (pH 7.0) at the scan rate of 100 mV/s: PDDA-HCNTs/MGCE (a), GOD–PDDA-HCNTs/MGCE (b) and GOD/MGCE (c). (B) The CVs of GOD–PDDA-HCNTs modified MGCE at scan rate of 50, 80, 100, 150, 200, 250, 300, 350, 400, 450, and 500 mV/s (from inner to outer curve) in nitrogen-saturated 0.10 M pH 7.0 PBS. Inset: plots of peak currents vs. scan rates.

electrode, which is not only beneficial the immobilization of enzymes, but also improve electron shuttle between the redox active sites of enzyme and the electrode.

It is well known that the direct electrochemistry of GOD is a two-electron coupled with two-proton reaction, which undergoes a redox reaction as follows [18]:

$$\mathrm{GOD-FAD} + 2\mathrm{e}^- + 2\mathrm{H}^+ \rightleftharpoons \mathrm{GOD-FADH_2} \quad (1)$$

Therefore, the pH value of the solution has influence on the electrochemical behavior of GOD on the PDDA-HCNTs/MGCE. Fig. 4 shows the CVs of the GOD–PDDA-HCNTs/MGCE in different pH solutions. Stable and well-defined CVs can be observed in the pH range of 4.0–8.0. An increase of solution pH caused a negative shift in both cathodic and anodic peak potentials. All changes in voltammetric peak potentials and currents with pH were reversible. For example, the CV for the GOD–PDDA-HCNTs/MGCE at pH 8.0 was reproduced after immersion in pH 4.0 buffer and then returned to the pH 8.0 buffer. The inset of Fig. 4 shows the effect of solution pH on the formal potential ($E^{0'}$) of the GOD–PDDA-HCNTs/MGCE, and it can be seen that the formal potential depends linearly on the pH value in the range of 4.0–8.0 with a slop of −57.3 mV/pH (R = 0.999), which is close to the theoretical value of −58.6 mV/pH according to the reaction shown in Eq. (1).

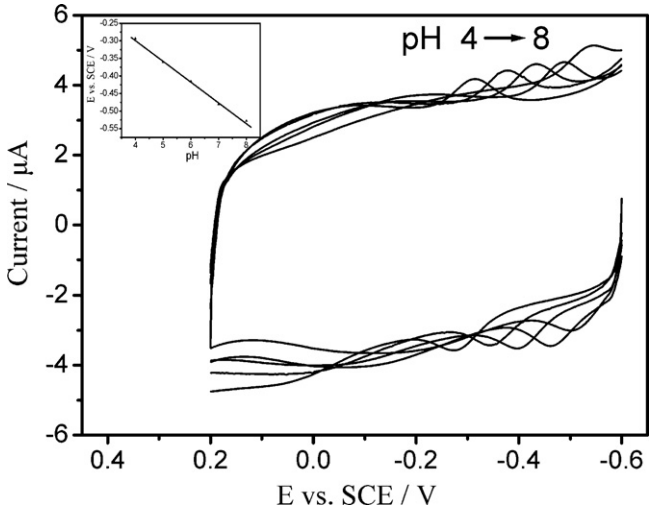

Fig. 4. The CVs of the GOD–PDDA-HCNTs/MGCE in different pH solutions.

3.3. Electrocatalytical behavior of the GOD–PDDA-HCNTs/MGCE

The effect of the dissolved oxygen on the electrochemical behavior of the GOD–PDDA-HCNTs/MGCE was investigated, as shown in Fig. 5A. Although a pair of well-defined, quasi-reversible redox peaks is observed in both deoxygenated and air-saturated PBS (pH 7.0), respectively, the reduction peak current of the GOD–PDDA-HCNTs/MGCE in air-saturated PBS is larger than that in deoxygenated PBS and the oxidation peak current is in reverse. The corresponding results are consistent with the previous reports [18,19]. It confirms that dioxygen dissolved in the solution is catalytically reduced at the GOD–PDDA-HCNTs/MGCE according to the following equations [18]:

$$\mathrm{GOD-FAD} + 2\mathrm{e}^- + 2\mathrm{H}^+ \rightleftharpoons \mathrm{GOD-FADH_2}$$

$$\mathrm{GOD-FADH_2} + \mathrm{O_2} \rightarrow \mathrm{GOD-FAD} + \mathrm{H_2O_2} \quad (2)$$

This is a typical EC catalytic process [20], in which oxygen regenerate GOD-FAD and enhance the reduction peak current of FAD. When glucose was added into this system, the reduction peak current decreased (curve b, Fig. 5A). The glucose restrained the electrocatalytic reaction due to the enzyme catalyzed reaction between GOD-FAD and glucose, which diminished the concentration of the GOD-FAD as shown in Eq. (3):

$$\mathrm{Glucose} + \mathrm{GOD-FAD} \rightarrow \mathrm{Gluconolactone} + \mathrm{GOD-FADH_2} \quad (3)$$

With the increasing glucose concentration, the peak current for the electrocatalytic reduction decreased, producing a glucose biosensor.

Fig. 5 depicts a current–time plot on successive step changes of glucose concentration at the applied potential of −0.50 V. The calibration curve for the biosensor under the optimized experimental conditions is shown in Fig. 5B. The biosensor displayed a linear response to glucose in the concentration range from 5 μM to 85 μM (R = 0.9988). The detection limit was estimated to be 0.72 μM at 3σ, which was obviously lower than that of the GOD/CNTs/GCE electrode reported in the literature previously (0.03 mM, S/N = 3) [21]. Furthermore, the sensitivity of GOD–PDDA-HCNTs/MGCE biosensor was calculated to be 174.0 μA mM^{-1} cm^{-2}, which was higher than 13.0, 1.06 and 0.053 μA mM^{-1} cm^{-2} for the glucose biosensors based on nitrogen-doped carbon nanotubes [22], single-walled carbon nanohorns [23] and highly ordered mesoporous carbon foams [24].

To assess the stability of GOD–PDDA-HCNTs/MGCE, the enzyme electrode was scanned continuously in a nitrogen-saturated PBS.

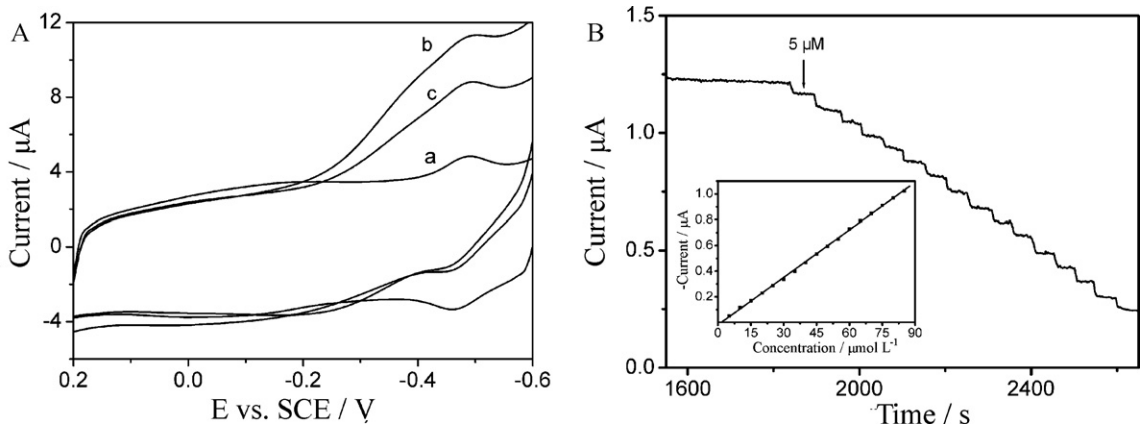

Fig. 5. (A) The CVs of the GOD–PDDA-HCNTs/MGCE in nitrogen-saturated 0.1 M pH 7.0 PBS (a), and the GOD–PDDA-HCNTs/MGCE in air-saturated 0.1 M pH 7.0 PBS in the (b) absence and (c) presence of 35 μM glucose. Scan rate: 100 mV/s. (B) Typical steady-state current response of the GOD–PDDA-HCNTs/MGCE on successive addition of 5 μM glucose into air-saturated PBS (pH 7.0). Applied potential: −0.5 V. The inset plot shows the linear calibration curve obtained at the biosensor.

After scanning for 50 cycles, the redox peak currents were essentially unchanged (by the comparison of the 50th cycle and the 2nd cycle). The prepared enzyme electrodes were stored in pH 7.0 PBS at 4 °C when it was not in use. The GOD–PDDA-HCNTs/MGCE could retain 95% of its initial response for glucose by cyclic voltammetry after 14-day storage, demonstrating excellent long-term stability. As for GOD–PDDA-HCNTs modified non-magnetic GCE, their response decreased to 50% of their initial response after only 3-day storage. The comparative results demonstrated that GOD–PDDA-HCNTs magnetically loaded on the magnetic GCE could better retain its enzymatic stability and bioactivity compared to that immobilized on the non-magnetic GCE. The interference with the response of GOD–PDDA-HCNTs/MGCE from ascorbic acid (AA) and uric acid (UA) was evaluated in pH 7.0 PBS in the presence of 25 μM glucose. It was found that the interference from 50 μM AA and UA was negligible. The excellent biosensing performance can be attributed to the combination of PDDA-HCNTs 3D-helical structure and its ferromagnetic property, which not only offered a biocompatible and stable surface for GOD loading, but also provided a sensitive electric interface for further biosensing.

4. Conclusions

In this work, PDDA-functionalized helical carbon nanotubes (PDDA-HCNTs) with good conductivity, ferromagnetic property, solubility and biocompatibility were successfully synthesized and firstly applied in GOD immobilization and biosensor construction. The results demonstrated that PDDA-HCNTs offered significant advantages in facilitating the electron transfer of immobilized enzymes and improving the biosensing performance of fabricated biosensors. Therefore, the studies have a significant potential impact on the selection of biosensing materials and on the design of electrochemical biosensors.

Acknowledgements

We greatly appreciate the support of the National Natural Science Foundation of China (20905010 and 51001019). This work is also supported by National Basic Research Program of China (2011CB933502), China Postdoctoral Science Foundation Funded Project (20100471293), the Fundamental Research Funds for the Central Universities (No. 1112020504), and the Changshu Institute of Technology (Thesis) team issue funded projects of China.

References

[1] X.L. Ren, X.W. Meng, D. Chen, F.Q. Tang, J. Jiao, Biosens. Bioelectron. 21 (2005) 433.
[2] Y. Xiao, F. Patolsky, E. Katz, J.F. Hainfeld, I. Willner, Science 299 (2003) 1877.
[3] Q. Xu, C. Mao, N.N. Liu, J.J. Zhu, J. Sheng, Biosens. Bioelectron. 22 (2006) 768.
[4] L. Bahshi, M. Frasconi, R.T. Vered, O. Yehezkeli, I. Willner, Anal. Chem. 21 (2008) 8253.
[5] A. Salimi, E. Sharifi, A. Noorbakhsh, S. Soltanian, Biosens. Bioelectron. 22 (2007) 3146.
[6] C.X. Cai, J. Chen, Anal. Biochem. 332 (2004) 75.
[7] C. Deng, J. Chen, X. Chen, Z. Xiao, S. Nie, Yao, Electrochem. Commun. 10 (2008) 907.
[8] R. Gill, L. Bahshi, R. Freeman, I. Willner, Angew. Chem. Int. Ed. 47 (2008) 1676.
[9] Y.C. Tsai, S.C. Li, J.M. Chen, Langmuir 21 (2005) 3653.
[10] S. Itoh, S. Ihara, J. Kitakami, Phys. Rev. B 47 (1993) 1703.
[11] S. Amelinckx, X.B. Zhang, D. Bernaerts, X.F. Zhang, V. Ivanov, J.B. Nagy, Science 265 (1994) 635.
[12] X.B. Zhang, X.F. Zhang, D. Bernaerts, G. Van Tendeloo, S. Amelinckx, J.V. Landuyt, V. Vanov, J.B. Nagy, P. Lambin, A.A. Lucas, Euro. Phys. Lett. 27 (1994) 141.
[13] N. Tang, W. Zhong, C. Au, Y. Yang, M. Han, K. Lin, Y. Du, J. Phys. Chem. C 112 (2008) 19316.
[14] N. Tang, W. Zhong, C. Au, A. Gedanken, Y. Yang, Y. Du, Adv. Funct. Mater. 17 (2007) 1542.
[15] N. Tang, J. Wen, Y. Zhang, F. Liu, K. Lin, Y. Du, ACS Nano 4 (2010) 241.
[16] G.Y. Zhang, X. Jiang, E.G. Wang, Appl. Phys. Lett. 84 (2004) 2646.
[17] J.D. Zhang, M.L. Feng, H. Tachikawa, Biosens. Bioelectron. 22 (2007) 3036.
[18] Q. Liu, X.B. Lu, J. Li, X. Yao, J.H. Li, Biosens. Bioelectron. 22 (2007) 3203.
[19] Y.X. Huang, W.J. Zhang, H. Xiao, G.X. Li, Biosens. Bioelectron. 21 (2005) 817.
[20] A.J. Bard, L.R. Faulkner, Electrochemical Methods: Fundamentals and Applications, 3rd ed., John Wiley & Sons, Inc., New York, 2001.
[21] J. Deng, X. Chen, C. Chen, L. Xiao, S. Nie, Yao, Biosens. Bioelectron. 23 (2008) 1272.
[22] S. Deng, G. Jian, J. Lei, Z. Hu, H. Ju, Biosens. Bioelectron. 25 (2009) 373.
[23] X. Liu, L. Shi, W. Niu, H. Li, G. Xu, Biosens. Bioelectron. 23 (2008) 1887.
[24] M. Zhou, L. Shang, B. Li, L. Huang, S. Dong, Biosens. Bioelectron. 24 (2008) 442.